New Phytologist

Handling the heat – photosynthetic thermal stress in tropical trees

Lasse Tarvainen[1], Maria Wittemann[1,2], Myriam Mujawamariya[1,2], Aloysie Manishimwe[1,2], Etienne Zibera[1,2], Bonaventure Ntirugulirwa[1,2,3], Claire Ract[1], Olivier J. L. Manzi[1,2], Mats X. Andersson[1], Cornelia Spetea[1], Donat Nsabimana[4], Göran Wallin[1] and Johan Uddling[1]

[1]Department of Biological and Environmental Sciences, University of Gothenburg, PO Box 461, Gothenburg SE-405 30, Sweden; [2]Department of Biology, University of Rwanda, University Avenue, PO Box 117, Huye, Rwanda; [3]Rwanda Agriculture and Animal Development Board, PO Box 5016, Kigali, Rwanda; [4]School of Forestry and Biodiversity and Biological Sciences, University of Rwanda, Busogo, Rwanda

Author for correspondence:
Lasse Tarvainen
Email: lasse.tarvainen@bioenv.gu.se

Received: *5 July 2021*
Accepted: *9 October 2021*

New Phytologist (2022) **233:** 236–250
doi: 10.1111/nph.17809

Key words: chlorophyll fluorescence, critical temperature, heat stress, photosystem II, thermal acclimation, thermal safety margin, thylakoid membrane lipids, tropics.

Summary

- Warming climate increases the risk for harmful leaf temperatures in terrestrial plants, causing heat stress and loss of productivity. The heat sensitivity may be particularly high in equatorial tropical tree species adapted to a thermally stable climate.
- Thermal thresholds of the photosynthetic system of sun-exposed leaves were investigated in three tropical montane tree species native to Rwanda with different growth and water use strategies (*Harungana montana*, *Syzygium guineense* and *Entandrophragma exselsum*). Measurements of chlorophyll fluorescence, leaf gas exchange, morphology, chemistry and temperature were made at three common gardens along an elevation/temperature gradient.
- Heat tolerance acclimated to maximum leaf temperature (T_{leaf}) across the species. At the warmest sites, the thermal threshold for normal function of photosystem II was exceeded in the species with the highest T_{leaf} despite their higher heat tolerance. This was not the case in the species with the highest transpiration rates and lowest T_{leaf}. The results point to two differently effective strategies for managing thermal stress: tolerance through physiological adjustment of leaf osmolality and thylakoid membrane lipid composition, or avoidance through morphological adaptation and transpiratory cooling.
- More severe photosynthetic heat stress in low-transpiring montane climax species may result in a competitive disadvantage compared to high-transpiring pioneer species with more efficient leaf cooling.

Introduction

Tropical forests have adapted to thermally stable conditions and thus may be particularly vulnerable to global warming (Janzen, 1967; Doughty & Goulden, 2008). This is concerning because the average, and even the coolest, tropical growing season temperatures of the late 21st Century have been predicted to exceed the hottest seasons recorded in the 20th Century (Battisti & Naylor, 2009; Diffenbaugh & Scherer, 2011). The global mean temperature increase is expected to occur in concert with both more intensive and frequent heatwaves (Coumou *et al.*, 2013; Perkins-Kirkpatrick & Lewis, 2020). This would potentially place many tropical plants under severe heat stress for extended periods. Already, increasing growth temperatures (T_g) have been linked to greater tree mortality and reduced woody productivity in the tropics (e.g. Toomey *et al.*, 2011; Aleixo *et al.*, 2019; Claeys *et al.*, 2019; Sullivan *et al.*, 2020). Warming also is an important driver of compositional changes towards greater dominance by warm-adapted species in high-elevation tropical forests (Duque *et al.*, 2015; Fadrique *et al.*, 2018). Although upward migration may provide montane species with temporary refuge from warming (Phillips, 1997; Feeley *et al.*, 2011), the benefits of moving upslope are partly counteracted by increased maximum radiation loads (e.g. Rosado *et al.*, 2016) that increase leaf temperatures (T_{leaf}) compared to plants growing at lower elevations (Fauset *et al.*, 2018). In addition, sufficiently fast migration may not be possible (Phillips, 1997; Feeley *et al.*, 2011) due to limitations on seed dispersal and unfavorable edaphic conditions (Duque *et al.*, 2015), which places emphasis on a species ability to handle high T_{leaf}. Overall, increased heat stress may profoundly affect the biodiversity of tropical forests, in particular by shrinking the distributional ranges of species that migrate too slowly and are unable to acclimate to the rapidly increasing temperatures.

The impact of increasing temperatures on leaf functioning depends on both the intensity and the duration of the heat exposure (Bilger *et al.*, 1984; Hüve *et al.*, 2011). Moderate heat stress can reduce carbon uptake through increases in mitochondrial

© 2021 The Authors
New Phytologist © 2021 New Phytologist Foundation
This is an open access article under the terms of the Creative Commons Attribution License, which permits use, distribution and reproduction in any medium, provided the original work is properly cited.

respiration and photorespiration, and reductions in stomatal conductance and photosynthesis that are transitory and cause the plant no long-term harm (Doughty & Goulden, 2008; Niinemets, 2018). An early sign of severe heat stress is the reduction of photosynthetic electron transport capacity, resulting from a loss of thylakoid membrane integrity and inactivation of the photosystem II (PSII) water-splitting complex (Hüve *et al.*, 2011; Teskey *et al.*, 2015; Yamamoto, 2016; Niinemets, 2018). Sufficiently long and/or large exceedance of heat tolerance thresholds leads to irreversible (or at least less reversible) damage to the photosynthetic biochemistry and leaf tissues (Berry & Björkman, 1980; Bilger *et al.*, 1984; Hüve *et al.*, 2011), with long-lasting impacts on plant-scale carbon (C) assimilation requiring senescence and production of new leaves to overcome.

Plants can reduce the risk for heat damage on leaves by two general strategies, avoidance and tolerance (e.g. Mathur *et al.*, 2014; Teskey *et al.*, 2015). Avoidance can occur through growth in the understory and/or through morphological adjustments on the plant- or the leaf-scale, such as shading of lower canopy leaves and having reflective leaves or leaf angles that reduce radiation loads, as well as by cooling of the leaf through transpiration (Leigh *et al.*, 2012; Michaletz *et al.*, 2015; Teskey *et al.*, 2015; Wright *et al.*, 2017; Drake *et al.*, 2018; Fauset *et al.*, 2018; Tserej & Feeley, 2021). These thermoregulatory traits act to maintain T_{leaf} in the optimal range for photosynthesis under normal environmental variation and help to avoid damage under more extreme conditions (Michaletz *et al.*, 2015; Fauset *et al.*, 2018). However, within-canopy variation in microclimate can cause T_{leaf} to vary by several degrees among species within the same stand or even among leaves within the same tree crown (e.g. Doughty & Goulden, 2008; Fauset *et al.*, 2018; Slot *et al.*, 2019). In addition to avoidance of high T_{leaf}, plants utilize several types of short- and long-term molecular and biochemical adjustments to increase their heat tolerance. These responses have been the topic of several recent reviews (Mathur *et al.*, 2014; Teskey *et al.*, 2015; Yamamoto, 2016) and include, but are not limited to, increased expression of heat shock proteins (Vierling, 1991; Barua *et al.*, 2003), increased production of osmolytes to improve protein stability (Santarius, 1973; Hüve *et al.*, 2006), and changes in the thylakoid membrane lipid composition towards greater saturation to reduce leakiness (Zhu *et al.*, 2018).

Several methods exist for investigating thermal tolerance thresholds, ranging from visual inspection of tissue damage to detailed analyses of thylakoid membrane composition and biochemical process rates. Because PSII function is among the most heat-sensitive photosynthetic components, chlorophyll fluorescence, which informs about the status of PSII (e.g. Maxwell & Johnson, 2000; Murchie & Lawson, 2013), has emerged as a common method for assessing leaf photosynthetic heat tolerance (PHT). Recently, it was shown globally using natural stands with varying species compositions, that the PHT threshold at which electron transport is disrupted due to increased thylakoid membrane fluidity and dissociation of membrane-bound proteins (often called T_{crit}) increased by 8°C over a span of 20°C difference in high-temperature extremes from the arctic to the tropics (O'Sullivan *et al.*, 2017). Similar relationships between threshold temperature and T_g have been found in multispecies studies with more constricted spatial scales and for single species under artificial warming (e.g. Knight & Ackerly, 2002; Drake *et al.*, 2018; Zhu *et al.*, 2018; Feeley *et al.*, 2020). However, this simple general picture of greater PHT thresholds in warm-adapted plants is complicated by observations of considerable among-species variation in the threshold temperatures in plants grown under similar thermal conditions (e.g. Knight & Ackerly, 2002; Curtis *et al.*, 2014; O'Sullivan *et al.*, 2017; Sastry & Barua, 2017; Feeley *et al.*, 2020).

Although it has been suggested that the photosynthetic thermal acclimation capacity is limited by the small day-to-day and seasonal variations in air temperature (T_{air}) experienced by tropical plants (Cunningham & Read, 2003; Doughty & Goulden, 2008), the acclimation of leaf PHT of tropical tree species has not been investigated systematically. In general, most field studies on PHT to date have either compared multiple species in a single common garden or used climatically differing stands with varying species compositions (however, see Knight & Ackerly, 2002, 2003, for a studies of congeneric perennial shrub species pairs from desert and coastal populations, and Krause *et al.*, 2010, for a study on tropical seedlings grown in open conditions compared to seedlings grown inside Aclar foil covered frames, which increased T_g by > 5°C). Detailed investigations into the within- and among-species variations in PHT and its acclimation capacity across T_g gradients are currently lacking from all biomes (Teskey *et al.*, 2015).

Studies on the differences between PHT thresholds and the high-temperature extremes experienced by plant leaves (thermal safety margin (TSM)) based on T_{air} have suggested that TSMs are greater in species with high PHT thresholds (O'Sullivan *et al.*, 2017; Sastry & Barua, 2017). However, recent findings based on measured and modelled T_{leaf} of tropical trees show PHT thresholds to be negatively correlated with TSMs (Perez & Feeley, 2020), and further that plants growing in the hottest climates already may be operating very near, or at, their thermal thresholds (Krause *et al.*, 2010; Perez & Feeley, 2020; Araújo *et al.*, 2021). Such differences in the estimated TSM trends highlight the importance of accounting for leaf thermoregulatory traits in analyses of PHT and the need for basing TSM evaluations on T_{leaf} rather than T_{air} to avoid overestimations (Pau *et al.*, 2018; Perez & Feeley, 2020; Slot *et al.*, 2021).

In this study we utilized three common gardens, all planted with seedlings propagated from common seed material, along an elevation/temperature gradient in Rwanda to investigate the acclimation capacity of PHT in three native tree species with different growth and water use strategies. The PHT thresholds were determined using a field-based chlorophyll fluorescence approach. These data were complemented with measurements on leaf gas exchange, morphology, chemistry and temperature, and energy balance-based modelling of long-term leaf temperatures to evaluate the following hypotheses:

(**1**) Tropical tree species with higher leaf temperatures have higher photosynthetic heat tolerance thresholds but exhibit smaller TSMs compared to species emphasizing heat avoidance strategies.

© 2021 The Authors
New Phytologist © 2021 New Phytologist Foundation

(**2**) Trees are able to acclimate photosynthetic heat tolerance thresholds in a warmer climate, but only partially (i.e. less than the change in T_g).
(**3**) The thermal acclimation of photosynthetic heat tolerance is linked to changes in leaf osmolality and thylakoid membrane lipid composition.

Materials and Methods

Definitions of the abbreviations used in the following sections are summarized in Table 1.

Field sites and plant material

The study was carried out on three field sites within the TRopical Elevational gradient Experiment in Rwanda (Rwanda TREE; see Mujawamariya *et al.*, 2021 for a detailed description) between 12 and 23 November 2018. The sites comprise a range of annual mean and maximum temperatures, and precipitation. The montane site, Sigira (2400 m above sea level (asl), Lat. 2°30′54″S, Long. 29°23′44″E), exhibits cool and wet conditions; 17.5°C/23.8°C mean/maximum daytime temperature, 2100 mm yr^{-1} precipitation and a soil texture ranging from clay to clay loam. The mid-elevation site, Rubona (1600 m asl, Lat. 2°28′30″S, Long. 29°46′49″E), is warmer and drier; 22.5°C/28.6°C mean/maximum daytime temperature, 1600 mm yr^{-1} precipitation, with soil texture ranging from clay to sandy clay loam. The lowest elevation site, Makera (1300 m asl, Lat. 2°6′31″S, Long. 30°51′16″E), is the warmest and driest site; 23.8°C/31.4°C mean/maximum daytime temperature, 1050 mm yr^{-1} precipitation, and has a soil texture ranging from clay loam to sandy clay loam. During periods with low precipitation, mainly in June to August 2018 irrigation corresponding to *c.* 25–30 mm per week was applied at all sites. The average soil water contents for the 30-d period before the measurements presented here were 28 ± 9% (v/v) at Sigira, 20 ± 4% at Rubona and 22 ± 5% at Makera (mean ± SD of six plots per site).

Each field site consists of 1800 native trees from 20 species. The trees are divided into 18 quadratic plots with in total 100 trees in each (i.e. five individuals per species), planted with a spacing of 1.5 m in December 2017–January 2018. The positions of tree individuals within each plot were randomized. The twenty species are divided among montane rainforest (10 species) and mid-elevation transitional rainforest (10 species), each group including species with both late and early successional life strategies. Since the measurements presented here were taken, the plots have been further divided into water and nutrient availability treatments but at the time of the current study all blocks at all sites were untreated, except for irrigation during dry periods to facilitate good establishment of the plantations. For this study, we selected three species with different water use strategies and leaf sizes (Supporting Information Table S1), and thus different expected leaf temperatures (T_{leaf}), based on gas exchange and morphological measurements from the sites. The chosen species were *Harungana montana* (*Hmo*), a high-transpiring montane pioneer-species with medium-sized leaves and an elevational distribution range from 2000 to 2400 m asl; *Syzygium guineense* (*Sgu*), a low-transpiring montane climax-species with small leaves found at elevations between 1350 and 2700 m asl; and *Entandrophragma exselsum* (*Eex*), a low-transpiring mid-elevation climax species with medium to large sized leaflets (denoted leaves hereafter) in compound leaves with an elevation range from 1500 to 2100 m asl (Bloesch *et al.*, 2009).

Table 1 List of abbreviations and their definitions.

Abbreviation	Definition	Unit
DBI	Double bond index	Count
DGDG	Digalactosyldiacylglycerol	–
E	Transpiration	mmol m^2 s^{-1}
Eex	*Entandrophragma exselsum*	–
F_m	Maximum fluorescence	Arbitrary
F_v	Variable fluorescence	Arbitrary
F_v/F_m	Maximum quantum efficiency of PSII	Ratio
F_0	Minimum fluorescence	Arbitrary
g_s	Stomatal conductance to water vapour	mol m^2 s^{-1}
Hmo	*Harungana montana*	–
MGDG	Monogalactosyldiacylglycerol	–
PG	Phosphatidylglycerol	–
PHT	Photosynthetic heat tolerance	–
PSII	Photosystem II	–
RH	Relative humidity	%
Sgu	*Syzygium guineense*	–
T_{air}	Air temperature	°C
T_{crit}	Critical temperature, T_{leaf} at which rapid F_0 increase starts	°C
T_{EB}	Leaf temperature calculated using the energy balance approach	°C
$T_{EBmean\text{-}max}$	The mean of the predicted daily leaf temperature maxima during the preceding 30 d (n = 30)	°C
T_{EBmax}	Mean of the five highest daily maximum leaf temperatures during the preceding 30 d (n = 5)	°C
T_g	Growth temperature, 30-d mean T_{air}	°C
T_{leaf}	Leaf temperature	°C
T_{20}	Leaf temperature at which F_v/F_m is reduced by 20% from an unstressed value	°C
T_{50}	Leaf temperature at which F_v/F_m is reduced by 50% from an unstressed value	°C
TSM	Thermal safety margin	°C

Chlorophyll fluorescence parameters

The among-species and -sites variations in photosynthetic heat tolerance (PHT) were investigated using chlorophyll fluorescence methodology (Maxwell & Johnson, 2000; Murchie & Lawson, 2013). With this approach the temperature response of PSII function is evaluated relative to either the minimum value of chlorophyll fluorescence (F_0), which gives a measure of the number of open reaction centers, or relative to the maximum quantum efficiency of PSII (F_v/F_m), where F_m is termed maximum fluorescence and represents chlorophyll fluorescence under short saturating light pulse when all reaction centers are closed. Variable fluorescence (F_v) is simply calculated as $F_m - F_0$.

© 2021 The Authors
New Phytologist © 2021 New Phytologist Foundation

A common way of expressing the heat tolerance threshold is the critical temperature at which F_0 increases rapidly (T_{crit}) or where F_v/F_m starts to rapidly decline. Another common measure is the temperature at which either the F_0 value is increased by, or the F_v/F_m value is reduced by, 50% compared to unstressed values (T_{50}). Throughout this study, T_{crit} refers to the T_{leaf} at which the rapid F_0 increase starts (Fig. S1), and T_{50} refers to the T_{leaf} at which F_v/F_m is reduced to half of its initial value (Fig. S2). In addition, we have determined T_{20}, the T_{leaf} at which F_v/F_m is reduced by 20% from its unstressed value (Fig. S2). We use this arbitrary threshold as an indicator of T_{leaf} where significant, but moderate, heat-induced reduction in photosynthetic function occurs. Notably, the absolute values of F_0 and F_m can be influenced by changes in leaf optical properties and the fraction of absorbed light received by PSII that may occur during stress treatments (Baker, 2008), and thus may provide biased estimates of the stress responses. However, the biasing effects cancel out when ratios, such as F_v/F_m, are considered (Baker, 2008).

Chlorophyll fluorescence measurements

Chlorophyll fluorescence was recorded on detached, dark-acclimated (for ≥ 30 min) leaves using a portable Pocket-PEA fluorimeter (Hansatech Instruments, King's Lynn, UK) with a light pulse of 3500 μmol photons m^{-2} s^{-1} and duration of 1 s. The instrument records data every 10 μs during measurement. The measurements were carried out inside huts at each field site. The leaves were collected pre-dawn and stored in envelopes in a plastic box (18–20°C throughout the day) when not measured. Wet paper towels were added to the box to maintain high humidity. Each leaf was first measured unheated at 20–25°C (depending on site and day), temperature which was low enough not to affect the measured fluorescence variables. Thereafter each leaf was dark-acclimated again in the plastic box and measured at only one higher temperature per collected leaf. This approach was chosen to avoid any potential lingering effects of heat stress from previous measurements. For each species and site, five to six leaves were measured at each higher temperature, with each leaf coming from a different and randomly selected plant. The overall temperature range spanned from 20 to 50°C, and included eight target temperatures (20–25, 30, 38, 42, 44, 46, 48 and 50°C).

The T_{leaf} was measured on the underside of the studied leaf using a 905i thermometer with a type K thermocouple (Testo, Lenzkirch, Germany) and controlled using infrared heating lamps (IR/PAR red 175W; Albert Kerbl GmbH, Buchbach, Germany) with dimmers. The T_{leaf} was recorded every 2 s and increased gradually to avoid overshooting the target temperature. The measurement was made when T_{leaf} was within ± 1°C of the target and had a maximum amplitude of variation of < 1°C for a 2-min period. Heating of the leaves took between 4 and 20 min depending on the target temperature. The rate of T_{leaf} increase thus was somewhat faster than the rate of 1°C min^{-1} commonly used in studies utilizing water baths. The temperature control worked well with the mean SD of the T_{leaf} during the 2-min periods at target temperature (60 readings taken at 2 s intervals) before the fluorescence measurements being 0.19°C averaged over all heated measurements, sites and species (n = 329). The setup during the measurements is shown in the (Fig. S3).

The effect of leaf detachment on the fluorescence parameters was tested by measurements at *c.* 20°C on dark-acclimated attached *Hmo* and *Sgu* leaves that subsequently were detached and re-measured following a new period of dark-acclimation. Neither F_0 nor F_v/F_m were significantly affected by detachment in either species (*Hmo*: P = 0.06 (F_0), P = 0.16 (F_v/F_m); *Sgu*: P = 0.72 (F_0), P = 0.66 (F_v/F_m), n = 6 for all, repeated measures ANOVA). In addition, the effect of duration of detachment on fluorescence parameters was tested by comparing measurements made on a set of leaves collected and measured at 30°C after dark-acclimation in the morning and another other set of leaves also collected in the morning and measured at 30°C, 5.5 h later. These measurements included leaves from all the studied species. As with detachment, neither F_0 nor F_v/F_m were significantly affected by the waiting time in any of the species (*Hmo*: P = 0.98 (F_0), P = 0.54 (F_v/F_m); *Sgu*: P = 0.18 (F_0), P = 0.42 (F_v/F_m); *Eex*: P = 0.54 (F_0), P = 0.32 (F_v/F_m), n = 5–6, one-way ANOVA).

In order to further test the performance of the chlorophyll fluorescence method, the acclimation of PHT thresholds was studied under controlled ambient conditions on *Hmo* seedlings grown in climate chambers (20°C : 15°C, 25°C : 20°C and 30°C : 25°C, day : night temperatures, operating on a 12:00 h : 12:00 h, light : dark photoperiod). In addition, the duration of impaired PSII function was tested using *Hmo* seedlings grown at 20°C : 15°C, day : night temperatures that were exposed to 2-min heat pulses at 42, 44 and 46°C. For a more detailed description of the methodology used for these analyses see Methods S1.

Leaf gas exchange and size

Leaf transpiration (E) and stomatal conductance to water vapour (g_s) were measured on attached leaves using two LI-6400 portable photosynthetic systems (Li-Cor Biosciences, Lincoln, NE, USA) in November 2018. The measurements for all species and sites were done at 25–30°C T_{leaf}, CO_2 concentration of 415 ppm, and saturating light conditions. Each combination of species and sites included five to six replicate plants. The relative humidity inside the measurement chamber was 50–80%. In order to obtain E and g_s values representative of the natural environment the gas exchange measurement were made *c.* 2 min after a leaf was inserted in the LI-6400 chamber, which is not sufficiently long for stomata to respond much to the chamber conditions. Leaf lengths and widths for 36 leaves (each from a separate plant) from each species and site were determined using a ruler and used for the energy balance-based determinations of long-term variation in leaf temperatures described below. In addition, in June 2019 the angles of fully developed outer canopy leaves (n = 14–15 per species at each site) were measured using a protractor (Table S1).

Thylakoid membrane lipid composition and osmolality

Several leaf discs were sampled from each plant used for the gas exchange measurements with a 10-mm punch. The sample

© 2021 The Authors
New Phytologist © 2021 New Phytologist Foundation

collection was carried out pre-dawn and the sampled discs were stored immediately in aluminum foil envelopes placed in a liquid nitrogen dry shipper (− 196°C). After transport to the laboratory, the samples were moved to a − 80°C freezer until extraction. Phase separation between chloroform ($CHCl_3$) and 2% acetic acid was used for extracting the thylakoid lipids from the leaf discs as described previously (Kourtchenko *et al.*, 2007). The thylakoid lipid composition was determined using liquid chromatography coupled to tandem mass spectrometry using an Agilent 1200 LC system coupled to either an Agilent 6470 Triple Quadrupole mass spectrometer or an Agilent 6410 triple quadrupole mass spectrometer (Agilent, Santa Clara, CA, USA). The lipids were separated using a C30 column and a solvent gradient as previously described (Nilsson *et al.*, 2019). The thylakoid lipid species were monitored using the transitions and settings described previously (Nilsson *et al.*, 2014). The total amounts of Monogalactosyldiacylglycerol (MGDG), digalactosyldiacylglycerol (DGDG) and phosphatidylglycerol (PG) were quantified as a sum of the species for each lipid class. Membrane stability was evaluated based on the average number of double bonds (the double bond index, DBI) in each lipid group; a decrease in DBI indicates a higher degree of saturation and increased membrane heat stability.

Osmolality was determined from leaf discs using a VAPRO 5600 vapor pressure osmometer (Wescor, Logan, UT, USA) following the protocol and equations provided by Bartlett *et al.* (2012) but with sampling of leaves pre-dawn instead of cutting, re-cutting and rehydrating branches in the lab.

Meteorological measurements

Each site is equipped with a climate station in the adjacent open field with half-hourly measurements of air temperature, relative humidity, photosynthetic photon flux density (PPFD), wind speed and direction, air pressure and accumulated precipitation. The measurements were made at 0.5 and 1.8 m aboveground, except for PPFD, wind speed and direction and precipitation, which were measured only at 1.8 m.

Leaf temperature modelling and observation

The half-hourly abiotic measurements, and leaf gas exchange and morphological data were used to simulate the temperature of a horizontal sun-exposed leaf (T_{EB}) with average g_s and leaf dimensions of each species using the energy balance approach (Campbell & Norman, 1998):

$$T_{EB} = T_{air} + \left[\frac{R_n - \lambda g_v D/p_a}{c_p g_{Hr} + \lambda s g_v}\right] \quad \text{Eqn 1}$$

(R_n, leaf incident net radiation; λ, latent heat of vaporization of water; g_v, vapor conductance; D, vapor pressure deficit; p_a, atmospheric pressure; c_p, specific heat of air; g_{Hr}, combined convective-radiative conductance; and s, slope of the saturation mole fraction function). For the R_n calculation, incoming short-wave radiation was converted from μmol m^{-2} to W m^{-2} using a conversion factor (4.6) and the clear sky emissivity was calculated according to Campbell & Norman (1998). Logarithmic wind profile was assumed when scaling wind speed to investigated leaf height (0.5 m or 1.8 m). The λ and the radiative conductance term of g_{Hr} were scaled to T_{air} (following Watson, 1943; Campbell & Norman, 1998, respectively). Lastly, the calculation of D accounted for the effect of p_a decrease with altitude on vapor pressure (Wang *et al.*, 2017). The energy balance calculation and the determination of the parameters is described in more detail in Methods S2.

At Sigira, the calculation was made for a leaf positioned at 0.5 m aboveground for all species. At Rubona and Makera, a leaf height of 0.5 m was used for *Sgu* and *Eex*, whereas 1.8 m was used for *Hmo*, based on measurements of tree heights in November 2018 (Table S1). The calculations were carried out for a 30-d period preceding the measurement campaign (14 October to 12 November), which was taken as representative of the T_g to which the plants were exposed.

In addition, T_{leaf} was measured at all sites in February 2019 using an infrared thermometer (Trotec BP10 IR; Trotec Laser GmbH, Ismaning, Germany). The observations were made on sunlit upper canopy leaves at midday to determine the peak T_{leaf} that the plants may reach under sunny and nondrought conditions.

Curve fitting and statistical analysis

The values of T_{crit}, T_{20} and T_{50} were determined by curve-fitting in SigmaPlot 12.5 (Systat Software, San Jose, CA, USA) on normalized data (i.e. with the value at 20–25°C designated as 1 for each leaf and the subsequent high temperature measurement expressed relative to this). We chose this approach to isolate the effect of heating on the chlorophyll fluorescence signal from any pre-treatment differences resulting from other possible stress factors that may have existed. However, it is unlikely that any other stress factors affected our findings regarding exceedance of the heat tolerance thresholds. The unheated F_v/F_m values (0.792 ± 0.002 mean ± SE, n = 355, pooled over all species and sites) indicated low levels of pre-treatment stress.

The T_{crit} was defined as the intersection point of two lines, representing the slow and rapid F_0 responses to increased T_{leaf}, using piecewise linear regression (Fig. S1). In order to calculate T_{20} and T_{50}, the F_v/F_m data were fitted against T_{leaf} using the Gompertz function (Fig. S2). We chose the Gompertz function over the commonly used simple logistics function because it does not assume symmetry with respect to how the fitted curve approaches the two asymptotes.

Because the fits were done on all available data the evaluations of the among-species and -sites differences were based on the degree of overlap of the SE of the fitted threshold temperatures and tested using the Welch's t-test. Specifically, the fitted parameters were considered significantly different when:

$$|x_1 - x_2| - 2.99 \times \sqrt{(SE_1^2 + SE_2^2)} > 0 \quad \text{Eqn 2}$$

© 2021 The Authors
New Phytologist © 2021 New Phytologist Foundation

(x_1 and x_2, two fitted threshold values (T_{crit}, T_{20} or T_{50}) being compared; SE_1 and SE_2, SE of the fit at these threshold values; and 2.99 is the *t*-score corresponding to $P = 0.05$ after adjustment to account for 18 multiple comparisons (three among-species comparisons × three sites + three among-sites comparisons × three species)).

Among-sites and -species variations in gas exchange variables, T_{leaf}, thylakoid membrane composition and osmolality were analyzed with two-way ANOVA in SPSS 25 (IBM Corp., Armonk, NY, USA). The data were log-transformed before the analysis in order to test multiplicative effects, and homogeneity of variances evaluated using the G-test ($\alpha = 0.05$, 't Lam, 2010). Tukey's honestly significant difference (HSD) test was used for *post hoc* analyses and Bonferroni correction was applied to account for multiple comparisons. In cases where significant site × species interactions were detected the individual effects of site and species were tested for using simple main effects analyses. To evaluate the acclimation of the threshold temperatures to peak T_{leaf}, we first calculated the mean of the five highest daily maximum leaf temperatures during the preceding month from the energy balance calculations (T_{EBmax}). We then used linear regression analysis to determine the correlations between T_{crit}, T_{20} or T_{50} and T_{EBmax} (SIGMAPLOT 12.5). The *F*-statistics for the analyses are included in Table S2.

Results

Climatic conditions

The air temperatures during the 30-d period before the measurements (Table 2) were similar to the longer-term data from the sites (see the Field sites and Plant Material section above). The weather conditions during the measurement days reflected the long-term and 30-d climate patterns (Fig. S4).

Stomatal conductance, transpiration and leaf temperature

Stomatal conductance and transpiration rate under reference conditions were significantly higher in the pioneer species *Hmo* than in the climax species *Sgu* and *Eex* ($P < 0.001$ for both; Fig. 1a,b). Neither process exhibited significant among-sites differences ($P = 0.14$ and $P = 0.17$ for g_s and E, respectively) or site × species interactions ($P = 0.055$ and $P = 0.20$ for g_s and E, respectively) (Fig. 1a,b).

Mean maximum daily T_{leaf} calculated using energy balance ($T_{EBmean\text{-}max}$), and the mean of the five highest daily maxima (T_{EBmax}), increased significantly from the high- to the low-elevation site across all species during the investigated 30-d period (Fig. 1c,d, respectively). At all sites, the leaves of the high-transpiring *Hmo* were cooler than those of *Eex,* whereas *Sgu* exhibited no clear pattern relative to the other species. Significant site × species interactions were detected in the predicted $T_{EBmean\text{-}max}$ and T_{EBmax} ($P < 0.001$ for both), reflecting a greater among-sites variation in *Eex* than in *Hmo* and *Sgu*. The energy balance-based T_{leaf} during the 30-d period before the thermal tolerance measurements (Fig. 1c,d) and the T_{leaf} measured in February 2019 (Fig. S5) exhibited similar among-sites and -species patterns.

Thylakoid membrane lipid composition and leaf osmolality

A decrease in mean DBI from the high- to the low-elevation site was detected in MGDG and DGDG across the species ($P < 0.001$, Fig. 2a,b). Among-species variation in DBIs was detected for all investigated lipid groups ($P \leq 0.003$, Fig. 2). Commonly, DBI was lower in *Eex* than in *Hmo*, with *Sgu* grouping with either of the other two species (Fig. 2). In addition, significant site × species interactions were detected for all lipid groups ($P \leq 0.04$; Fig. 2) indicating that the pattern of lipid composition adjustments to higher T_g varied among the species. Notably, low transpiration rates (Fig. 1b) and high T_{leaf} (Fig. 1c,d) coincided with low DBIs (Fig. 2), thereby linking leaf cooling efficiency and membrane heat stability (i.e. thermal tolerance) to the T_{leaf} experienced by the trees. Osmolality did not vary among the sites for any species ($P = 0.56$; Fig. 3) but was significantly higher in *Eex* than in *Sgu* and *Hmo* ($P < 0.001$).

Among-sites and -species variation in leaf temperature thresholds

The T_{crit} of *Eex* was greater at the low-elevation site than at the high- and mid-elevation sites ($P < 0.05$; Fig. 4a). It also was greater than the T_{crit} of *Hmo* and *Sgu* at the low-elevation site ($P < 0.05$; Fig. 4a). No other significant among-sites or -species differences were detected in T_{crit}.

Table 2 Air temperature (T_{air}, °C), daytime air temperature (T_{air_day}, °C), maximum air temperature (T_{air_max}, °C), daytime photosynthetic photon flux density ($PPFD_{day}$, μmol m^{-2} s^{-1}), relative humidity (RH, %) and total precipitation (mm) measured half-hourly at 1.8 m aboveground during the 30 d before the start of measurement campaign (14 October 2014–12 November 2018).

Site	T_{air} (°C)	T_{air_day} (°C)	T_{air_max} (°C)	$PPFD_{day}$ (μmol m^{-2} s^{-1})	RH (%)	Precipitation (mm)
Sigira	15.1 ± 0.1	16.7 ± 0.1	20.8 ± 0.3 (23.3)	577 ± 18	82.5 ± 0.3	242
Rubona	20.0 ± 0.1	22.1 ± 0.1	26.3 ± 0.2 (28.7)	818 ± 23	74.9 ± 0.3	67
Makera	20.5 ± 0.1	23.6 ± 0.2	28.5 ± 0.4 (31.7)	729 ± 22	80.0 ± 0.4	171

The 24-h means ± SE are shown for T_{air}, and RH (n = 1437–1440). Mean ± SE T_{air_day} and $PPFD_{day}$ were calculated for 06:00–18:00 h (when PPFD > 0, n = 748–750). For T_{air_max} both the mean ± SE of the daily maxima (n = 30) and the absolute maxima during the 30-d period (value in parentheses) are shown.

© 2021 The Authors
New Phytologist © 2021 New Phytologist Foundation

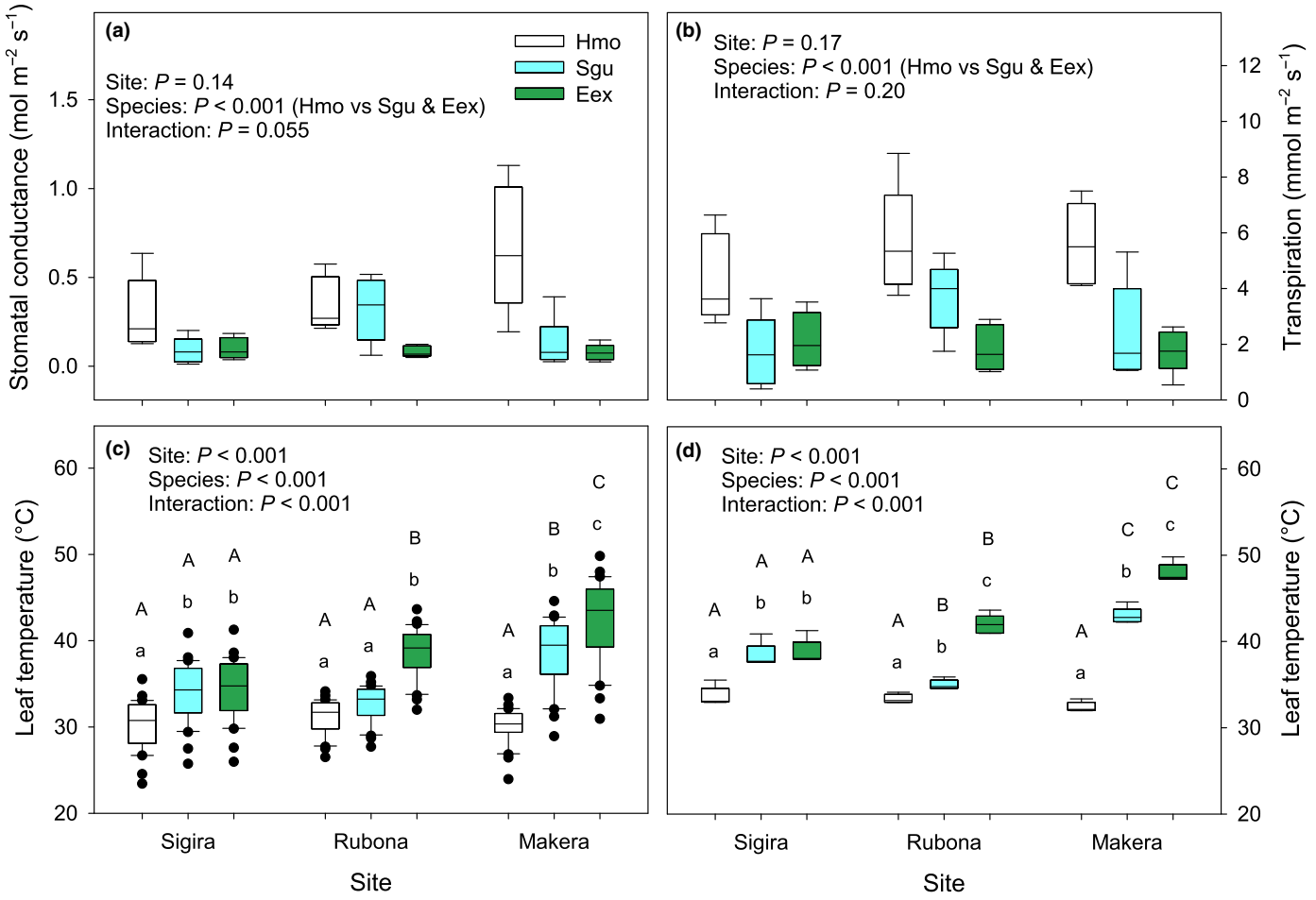


Fig. 1 Among-sites and -species variation in (a) stomatal conductance (mol m^{-2} s^{-1}, n = 5–6), (b) leaf transpiration (mmol m^{-2} s^{-1}, n = 5–6), (c) mean maximum daily leaf temperature during the 30-d period before measurements calculated using energy balance (°C, n = 30, statistics), and (d) the mean of the five highest maximum daily leaf temperatures during the period (°C, n = 5, T_{EBmax} in Fig. 5). The median (central line of the box), the 75th percentile (upper line), 25th percentile (lower line), and the 90th and the 10th percentiles (whiskers) are shown. Dots indicate data points outside the 10th and the 90th percentiles. *Hmo*, *Harungana montana* (white); *Sgu*, *Syzygium guineense* (cyan); *Eex*, *Entandrophragma exselsum* (green). Upper case letters indicate significant among-sites differences within each species, and lower case letters indicate significant among-species differences within each site. In (a) and (b) the *post hoc* analysis on species differences (*Hmo* vs *Sgu* and *Eex*) was based on the entire dataset because the interaction term was not significant.

For all species, T_{20} and T_{50} were greater at the low- than at the high-elevation site (P < 0.05; Fig. 4b,c). For *Eex*, both T_{20} and T_{50} were lower at the mid-elevation site than at the low-elevation site. For *Sgu*, T_{20} and T_{50} at the mid-elevation site were intermediate to the values observed at the low- and high-elevation sites. For *Hmo*, T_{50} at the mid-elevation site was greater than at the high-elevation site. With respect to among-species variation, both T_{20} and T_{50} were higher in *Eex* than in *Hmo* and *Sgu* at the high-elevation site (P < 0.05; Fig. 4b,c). At the mid-elevation site, T_{50} of *Sgu* was significantly lower than that of *Eex*. At the low-elevation site, T_{20} was lower in *Hmo* than in *Sgu* and *Eex*, and all species had T_{50} values that were significantly different from each other (P < 0.05; Fig. 4b,c).

T_{crit} correlated more strongly with the DBI of PG (r^2 = 0.41, P = 0.065) than the DBIs of MGDG (r^2 = 0.11, P = 0.38) and DGDG (r^2 = 0.05, P = 0.56) (linear regressions fitted on data pooled from all sites and species, n = 9; Fig. S6). The T_{50} (r^2= 0.73, P = 0.003) was strongly correlated with DBI of MGDG (Fig. S6), whereas T_{20} (r^2 = 0.39, P = 0.07) was not (Fig. S6). The correlations with the DBIs of PG (T_{20}, r^2 = 0.28, P = 0.15; T_{50}, r^2 = 0.30, P = 0.13) and DGDG (T_{20}, r^2 = 0.25, P = 0.17; T_{50}, r^2 = 0.17, P = 0.28) were weak (n = 9 for all; Fig. S6).

In the climate chamber-grown *Hmo* seedlings, all threshold parameters acclimated to growth temperature (20°C : 15°C, 25°C : 20°C and 30°C : 25°C, day : night) (Fig. S7; n = 6; T_{crit}, P = 0.044; T_{20}, P < 0.001; and T_{50}, P = 0.001). In addition, the threshold temperatures under all growth temperatures were greater in chamber-grown plants that those observed in the field-grown plants.

Exceedance and acclimation of heat tolerance thresholds

The horizontal distances between the T_{EBmax} values and the 1 : 1 line in Fig. 5(a–c) can be interpreted as species- and site-specific TSMs. During the 30-d growth period, daily maximum T_{EB} (Eqn 1) exceeded T_{crit} and T_{20} in *Eex* at the high-elevation (T_{crit} 1/30 d,

© 2021 The Authors
New Phytologist © 2021 New Phytologist Foundation

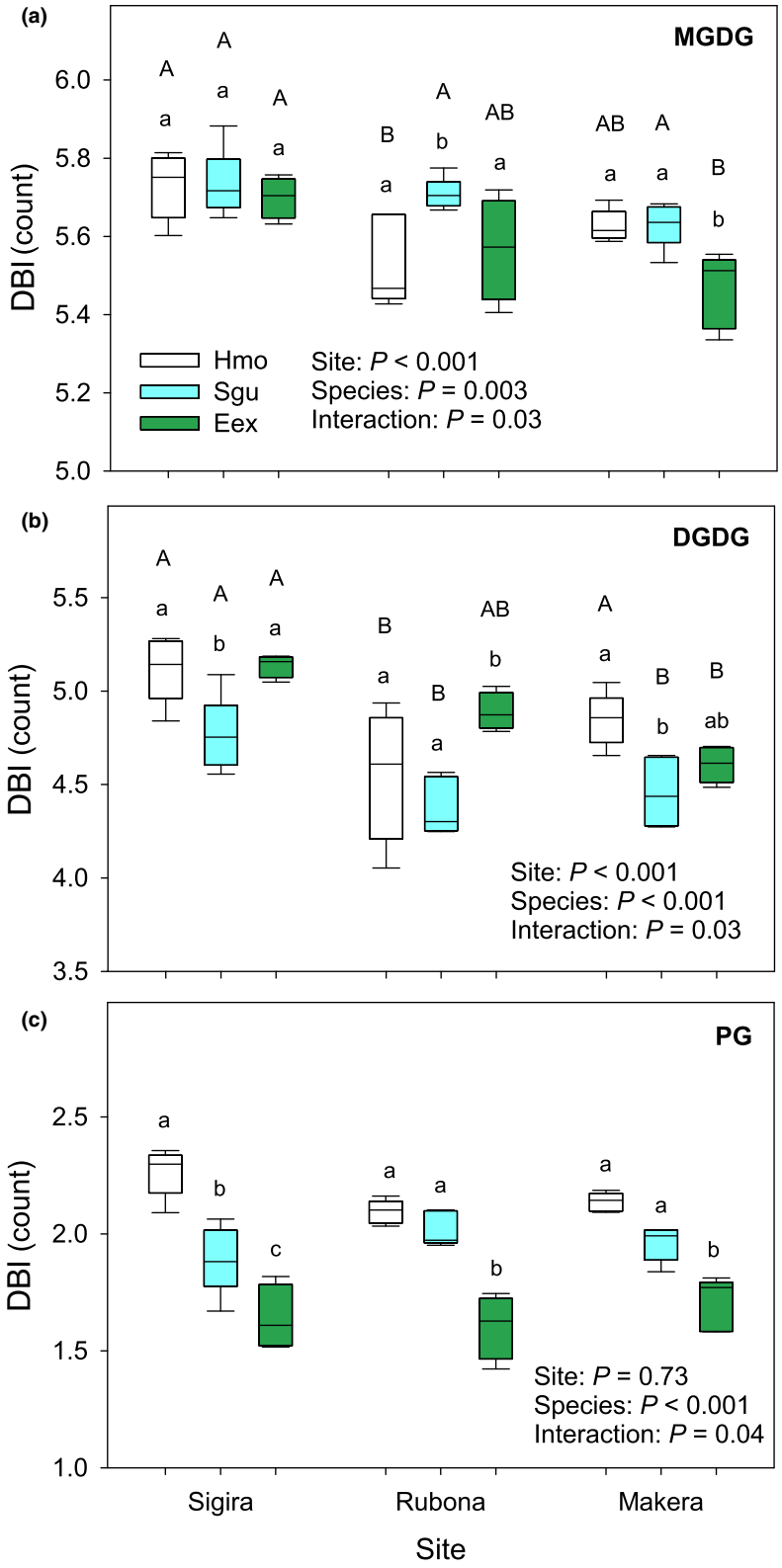


Fig. 2 Among-sites and -species variation in thylakoid membrane lipid composition with respect to the double bond index (DBI, count) for the lipid classes (a) Monogalactosyldiacylglycerol (MGDG), (b) Digalactosyldiacylglycerol (DGDG) and (c) Phosphatidylglycerol (PG). The median (central line of the box), the 75th percentile (upper line), 25th percentile (lower line), and the 90th and the 10th percentiles (whiskers) are shown. *Hmo*, *Harungana montana* (white); *Sgu*, *Syzygium guineense* (cyan); *Eex*, *Entandrophragma exselsum* (green). Upper case letters indicate significant among-sites differences within each species. Lower case letters indicate significant among-species differences within each site.

T_{20} 1/30 d), mid-elevation (T_{crit} 3/30 d, T_{20} 3/30 d) and low-elevation (T_{crit} 13/30 d, T_{20} 15/30 d) sites (Fig. 5a,b). The T_{50} threshold was exceeded in *Eex* at the low-elevation site (6/30 d; Fig. 5c). In *Sgu*, T_{crit} and T_{20} were exceeded at the high-elevation (T_{crit} 1/30 d, T_{20} 1/30 d) and low-elevation (T_{crit} 8/30 d, T_{20} 2/30 d) sites (Fig. 5a,b). In the high-transpiring pioneer-species, *Hmo*, the daily T_{leaf} maxima were below the PHT thresholds during the entire 30-d period at all sites (Fig. 5a–c). Both T_{20} and T_{50} increased significantly with T_{EBmax} (regression lines fitted to pooled data in Fig. 5b,c) indicating thermal acclimation corresponding to 0.29°C

© 2021 The Authors
New Phytologist © 2021 New Phytologist Foundation

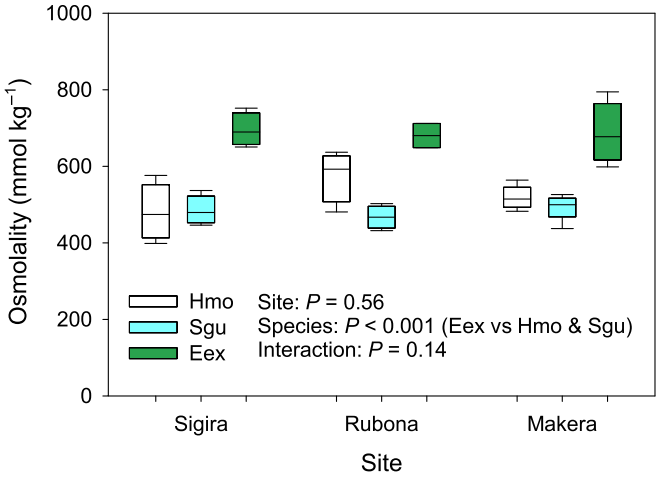


Fig. 3 Among-sites and -species variation in leaf osmolality (mmol kg^{-1}). The median (central line of the box), the 75th percentile (upper line), 25th percentile (lower line), and the 90th and the 10th percentiles (whiskers) are shown. *Hmo*, *Harungana montana* (white); *Sgu*, *Syzygium guineense* (cyan); *Eex*, *Entandrophragma exselsum* (green). The *post hoc* analysis on species differences (*Eex* vs *Hmo* and *Sgu*) was based on the entire dataset because the interaction term was not significant.

T_{20}°C^{-1} T_{EBmax} (r^2 = 0.52, P = 0.029) and 0.25°C T_{50}°C^{-1} T_{EBmax} (r^2 = 0.54, P = 0.023), respectively.

Recovery from heat exposure

The duration of the recovery of the maximum quantum efficiency of PSII (i.e. F_v/F_m) from a 2-min heat pulse was strongly dependent on the intensity of the heating. The F_v/F_m of chamber-grown (20°C : 15°C, day : night) *Hmo* plants was reduced to 76% of the pre-treatment value by a heat pulse at 42°C, and recovered fully within 8 h. Almost full recovery from an initial F_v/F_m reduction to 60% was observed after 120 h following a heat pulse at 44°C. By contrast, a heat pulse at 46°C reduced F_v/F_m to 18% of its pre-treatment value and it recovered to only 62% during the 120-h experiment indicating irreversible damage of the PSII complex (Fig. 6). Regardless of the heat pulse intensity, the F_v/F_m reduction was the strongest during the heating. A rapid initial recovery occurred during the first 30 min and was followed by a more gradual increase in F_v/F_m (Fig. 6).

Discussion

We utilized common gardens established along an elevation/temperature gradient in central Africa (Rwanda) to explore the among-species differences in, and the thermal acclimation potential of, photosynthetic heat tolerance (PHT) thresholds in three tropical montane tree species. The low-transpiring climax species, *Entandrophragma exselsum* (*Eex*), experienced the highest leaf temperature (T_{leaf}) and had both the highest PHT thresholds and the narrowest TSMs, whereas the opposite was true for the high-transpiring pioneer species *Harungana montana* (*Hmo*) (Hypothesis 1). All of the tested species were able to partially acclimate their PHT to increasing growth

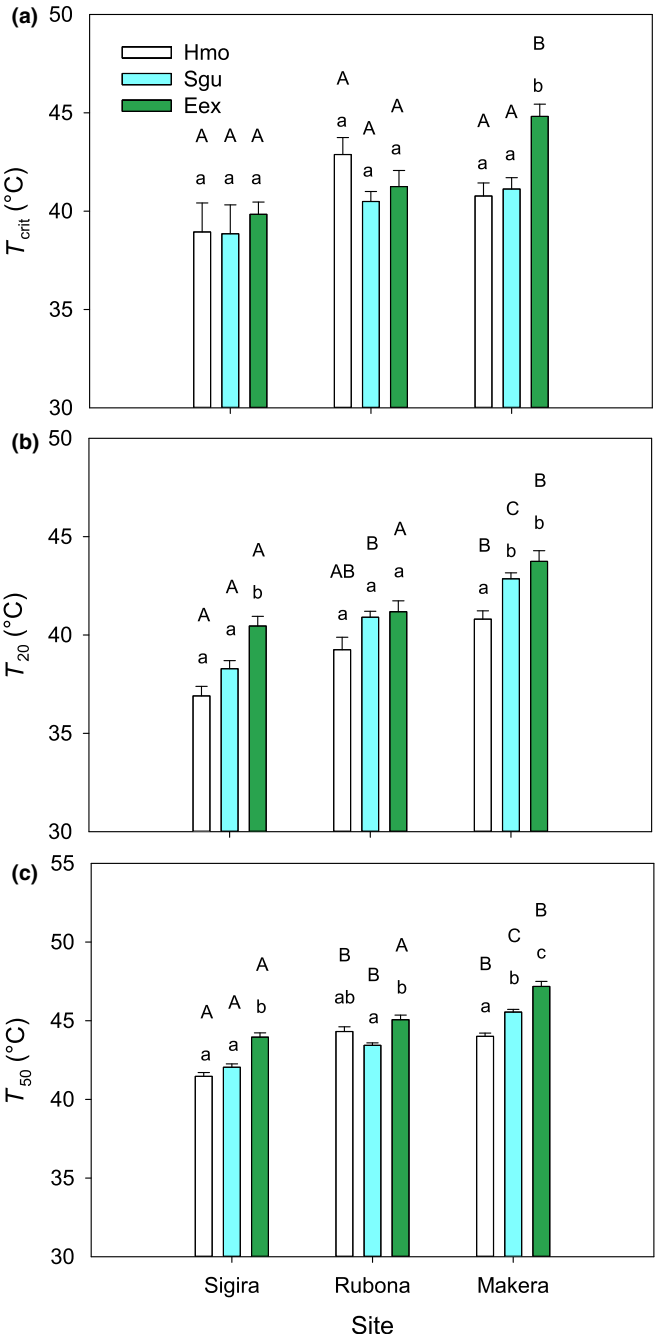


Fig. 4 Among-sites and -species variation in (a) critical temperature (T_{crit}, °C) and the temperatures at which the F_v/F_m is reduced by (b) 20% (T_{20}, °C) and (c) 50% (T_{50}, °C) compared to nonheat stressed conditions. *Hmo*, *Harungana montana* (white); *Sgu*, *Syzygium guineense* (cyan); *Eex*, *Entandrophragma exselsum* (green). Data are shown as mean ± SE of the fitted temperature values. Upper case letters indicate significant among-sites differences within each species (P = 0.05). Lower case letters indicate significant among-species differences within each site (P = 0.05). The statistical comparisons among the groups were made using Welch's t-tests and are detailed in Supporting Information Tables S3–S5.

temperatures (T_g) (Hypothesis 2). Leaf osmolality did not acclimate to T_g but was the highest in the most heat-tolerant species, suggesting that high osmolality may be inherently beneficial for heat tolerance. By contrast, the saturation level of

© 2021 The Authors
New Phytologist © 2021 New Phytologist Foundation

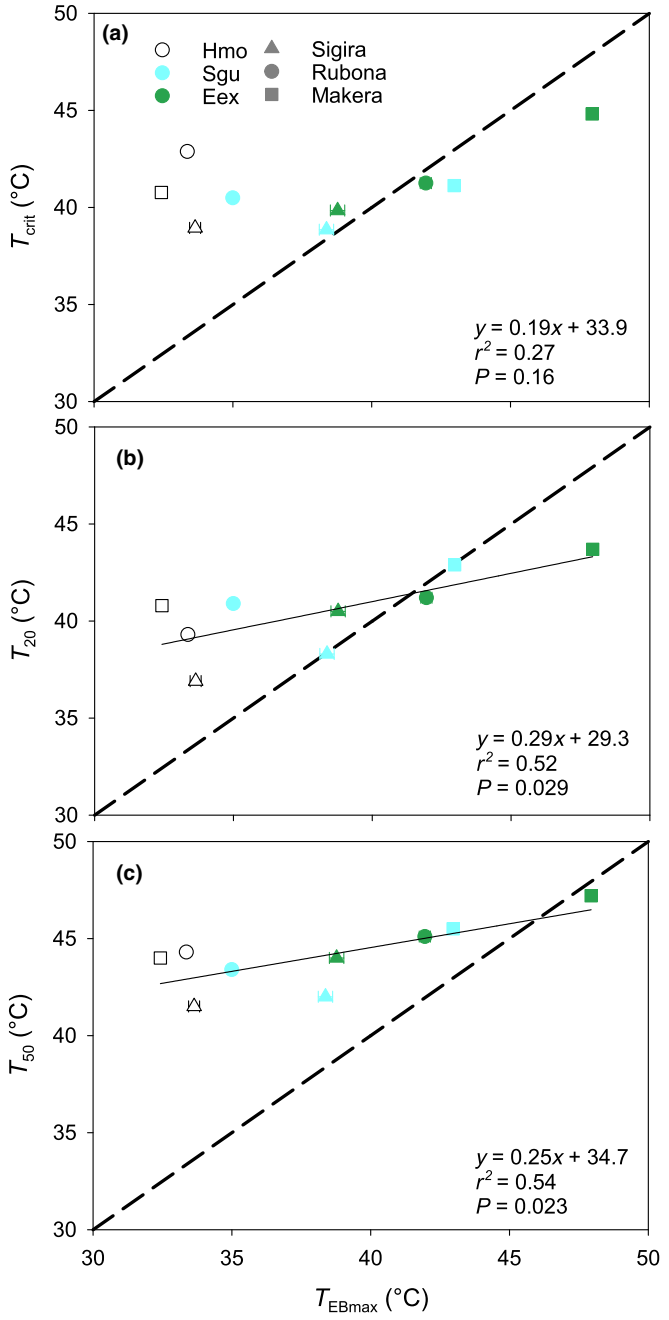


Fig. 5 Variation in (a) critical temperature (T_{crit}, °C), and the temperatures at which the F_v/F_m is reduced by (b) 20% (T_{20}, °C) and (c) 50% (T_{50}, °C) plotted against the mean of the five highest maximum daily leaf temperature from energy balance modelling (T_{EBmax}). *Hmo*, *Harungana montana* (white); *Sgu*, *Syzygium guineense* (cyan); *Eex*, *Entandrophragma exselsum* (green). Triangles, Sigira (high-elevation site); circles, Rubona (mid-elevation site); and squares, Makera (low-elevation site). Values below the 1 : 1 line indicate exceedance of the given temperature tolerance threshold. In (b) and (c) significant slopes of the regression lines fitted to the pooled data indicate the response of T_{20} and T_{50} to prevailing maximum leaf temperatures, respectively, (°C T_x °C^{-1} T_{EBmax}). The pooled T_{crit} data were not significantly related to T_{EBmax}.

thylakoid membrane lipids increased with increasing T_g in all species, indicating clear thermal acclimation in this trait (Hypothesis 3).

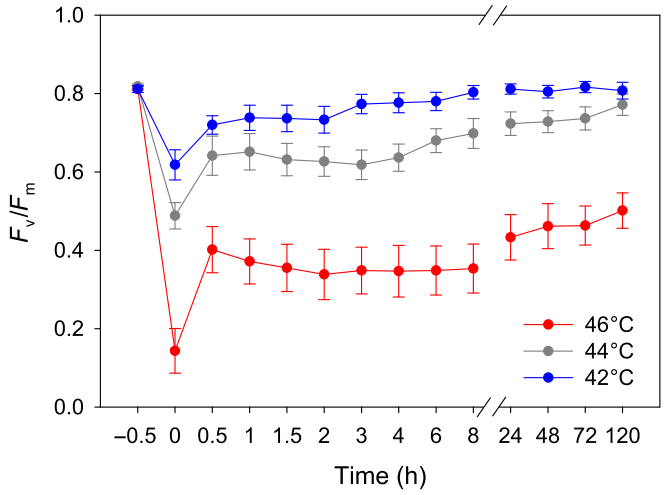


Fig. 6 The recovery of dark-adapted F_v/F_m signal from a 2-min heat pulse at 42, 44 and 46°C in leaves of chamber-grown *Harungana montana* over 120 h following heat exposure. The heat pulse was administered at 0 h. Means ± SE are shown.

Photosynthetic heat tolerance and acclimation

The observed rate of T_{50} (T_{leaf} at which fluorescence is reduced by 50% compared to unstressed values) increase with increasing T_g, 0.25°C °C^{-1} T_{EBmax} (daily maximum leaf temperatures from the energy balance calculations), across the studied species (Fig. 5c) is comparable to other estimates of PHT acclimation (O'Sullivan *et al.*, 2017; Drake *et al.*, 2018; Zhu *et al.*, 2018; Slot *et al.*, 2021). Like Perez & Feeley (2020), we saw no general T_{crit} (T_{leaf} at which the minimum value of chlorophyll fluorescence starts to increase rapidly) acclimation across species (Fig. 5a). However, the T_{crit} of *Eex* was significantly higher at the warmest site than at the two cooler sites (Fig. 4a).

The current study explored potential roles for leaf osmolality and thylakoid membrane lipids as biochemical drivers of PHT based on previous work highlighting their importance for thermal acclimation (Hüve *et al.*, 2006; Mathur *et al.*, 2014; Zhu *et al.*, 2018). Although the current study offers only a snapshot of the osmolality in the studied trees, the high values observed in the heat-tolerant *Eex* combined with a lack of among-sites acclimation in any species (Fig. 3) suggest that high osmolality may be a species-level adaptive trait promoting greater PHT that does not readily acclimate to T_g. Thylakoid membrane lipid saturation level, however, acclimated to T_g in all species (Fig. 2), which agrees with the previous observation of a positive correlation between PHT and abundance of saturated fatty acids that promote membrane stability (Zhu *et al.*, 2018). Other processes not studied here, such as production of isoprenes and heat shock proteins, also may contribute to heat acclimation (Sharkey, 2005; Teskey *et al.*, 2015; Aspinwall *et al.*, 2019; Pollastrini *et al.*, 2019; Taylor *et al.*, 2019; Rodrigues *et al.*, 2020). Future studies including these processes may offer greater insight into their direct effects on the among-species variation in PHT and its acclimation capacity in tropical trees.

Overall, species utilizing the high-tolerance strategy, such as *Eex*, would appear to benefit from having high capacity for PHT

© 2021 The Authors
New Phytologist © 2021 New Phytologist Foundation

acclimation because of their generally high T_{leaf} and generally narrow TSMs (Fig. 5; Perez & Feeley, 2020). By contrast, investing in PHT acclimation capacity may be energetically wasteful in species such as *Hmo*, with traits promoting lower T_{leaf} through efficient thermoregulation (Michaletz *et al.*, 2015, 2016; Fauset *et al.*, 2018). The findings of the current study, together with the covariation observed among leaf traits, energetics and PHT (Michaletz *et al.*, 2015, 2016; Sastry & Barua, 2017; Fauset *et al.*, 2018; Araújo *et al.*, 2021; Slot *et al.*, 2021), suggest that trait-based approaches (e.g. Wright *et al.*, 2004; Reich, 2014) could be useful for inferring not only a species' intrinsic PHT, but also its acclimation capacity.

Thermal safety margins

We found that TSMs were narrower in species with high T_{leaf}, despite their higher T_{20} (T_{leaf} at which fluorescence is reduced by 20% from its unstressed value) and T_{50} (Fig. 5, horizontal distance to 1 : 1 line). Exceedance of T_{20} was common in *Eex* at the mid- and low-elevation sites and in *Syzygium guineense* (*Sgu*) at the high- and low-elevation sites. In addition, T_{50} exceedance was common in *Eex* at the low-elevation site. These results thus agree with the suggestion that plants in the hottest environments may be operating close to their thermal limits (Krause *et al.*, 2010; Perez & Feeley, 2020). Furthermore, our observations agree with a previous report showing that T_{leaf}-based TSMs are the narrowest in tropical species with the highest T_{50} (Perez & Feeley, 2020). This contrasts with studies based on T_{air} that have commonly found TSMs to be the widest in species with high PHT thresholds (O'Sullivan *et al.*, 2017; Sastry & Barua, 2017) and further emphasizes the importance of using T_{leaf} rather than T_{air} when evaluating TSMs (Pau *et al.*, 2018; Perez & Feeley, 2020).

Tropical tree species tend to group in microhabitats and leaf microclimate has been indicated as a potentially more important driver of PHT acclimation than overall T_g (Curtis *et al.*, 2019). Likewise, it has been suggested that species may be selectively distributed to hotter or cooler microhabitats based on their thermal tolerance (Feeley *et al.*, 2020). Although such grouping effects were excluded by the randomized planting design in the current study, clearly species that use latent cooling to regulate T_{leaf} under heat exposure would benefit from growing under wetter conditions. Climate change is expected to be accompanied by intensification of droughts and greater vapor pressure deficits (Allen *et al.*, 2010; Teskey *et al.*, 2015). Using transpiration to retain wide TSMs, like *Hmo* in this study, may thus become increasingly difficult due to the trade-off that exists between thermoregulation and hydraulic safety (Fauset *et al.*, 2018, but see Drake *et al.*, 2018). This is illustrated by the large impact transpiration had on the energy balance-based T_{leaf} estimates for *Hmo* compared to *Eex* at the warmest site. For *Hmo*, using observed g_s (0.67 ± 0.16 mol m^2 s^{-1}, mean ± SE, n = 5) yielded a T_{EBmax} estimate of 32.4 ± 0.1°C (mean ± SE, n = 5; Fig. 5), whereas using g_s = 0 mol m^2 s^{-1} (i.e. excluding latent cooling) yielded an estimate of 46.9 ± 0.2°C (mean ± SE, n = 5), which is higher than the observed T_{50} (44.0°C; Fig. 4). For *Eex*, T_{EBmax} calculation with g_s = 0 mol m^2 s^{-1} yielded an estimate of 54.8 ± 0.2°C (mean ± SE, n = 5) compared to 47.9 ± 0.2°C (mean ± SE, n = 5) with observed g_s (0.08 ± 0.02 mol m^2 s^{-1}, mean ± SE, n = 5). As *Hmo* and *Eex* have similar-sized leaves (Table S1), the remaining difference was due to leaf height (1.8 and 0.5 m, respectively) used in the modelling, mainly through its impact on wind speed. As reduced water availability during heat stress could tip the competitive balance towards species relying on the tolerance strategy, such as *Eex*, future studies exploring temperature and drought interactions would appear especially valuable.

When evaluating the energy balance-based estimates of T_{leaf} presented here, it should be noted that we made two important simplifying assumptions that affect our findings. First, we modelled horizontal unshaded leaves, whereas natural canopies exhibit a wide range of leaf angles and light availabilities. Both shading and steep leaf angles reduce radiation interception and, thus, generally lead to lower T_{leaf}. However, during the early afternoon when T_{air} is the highest and the Sun has passed zenith, the leaf angles observed at the field sites for outer canopy leaves (*c.* 20° averaged over species and sites; Table S1) are such that incoming solar radiation would be near perpendicular to these leaves (Ntawuhiganayo *et al.*, 2020). Thus, the estimates of the daily maximum T_{leaf}, which were the point of interest for this study, were likely not much affected by this assumption. A similar conclusion was reached by Perez & Feeley (2020) who used theoretical and observed probability distributions of leaf angles to show that a non-negligible proportion of leaves in canopies are horizontal or have angles ≤ 15°, which corresponds to < 1°C of cooling compared to horizontal when the Sun is at zenith.

The second simplifying assumption was the use of constant g_s values for the entire 30-d period for which the energy balance-based modelling was carried out. Cooling by transpiration is an important part of leaf thermoregulation (e.g. Drake *et al.*, 2018; Fauset *et al.*, 2018), and both g_s and transpiration can vary strongly seasonally and within a given day. In this study, any significant long-term variation in transpiration potential was unlikely given that the meteorological conditions during the modelled 30-d period were stable (Table 2) and irrigation was applied at the mid- and low-elevation sites to ensure that the trees were not water-stressed. Given this meteorological stability it also is likely that other traits promoting the tolerance or avoidance strategies, such as leaf angles, did not change much during the modelled period. Furthermore, the gas exchange measurements were made over the day (*c.* 09:00 h–16:30 h) and would have captured the daytime variation in g_s. We note, however, that using the daytime average likely resulted in an overestimation of the g_s during the warmest hour of the day, which would have led to some underestimation of T_{leaf} with the energy balance-based approach.

Observed photosynthetic heat tolerance thresholds compared to previous studies

We note that the PHT thresholds observed in the current study are in the lower end of the range reported for tropical tree species: for T_{crit} from *c.* 46–50°C, and for T_{50} from *c.* 44.5–53°C (e.g.

© 2021 The Authors
New Phytologist © 2021 New Phytologist Foundation

Sastry & Barua, 2017; Zhu *et al.*, 2018; Feeley *et al.*, 2020; Perez & Feeley, 2020; Tiwari *et al.*, 2021; Slot *et al.*, 2021). Given that our laboratory-based measurements on *Hmo* also yielded higher threshold values in the higher temperature treatments (i.e. at 25°C : 20°C and 30°C : 25°C, day : night; Fig. S7) this may simply reflect the rather low mean temperatures at our field sites (15–20°C) compared to the more studied lowland tropics (Slot *et al.*, 2021). Furthermore, our low PHT thresholds in the field compared to previous studies also may be caused by differences in measurement protocols. In our study, the chlorophyll fluorescence measurements were made directly after the heat pulse. Such measurements are likely to yield lower threshold estimates than the commonly used protocol of Krause *et al.* (2010) where the measurements are made 24–48 h after the heat exposure. This is related to a rapid partial recovery of PSII function following heat stress (Fig. 6; Krause *et al.*, 2010). The rapid recovery occurs because some of the initial reduction is associated with transient processes caused by production of reactive oxygen species (ROS) in response to heat-induced functional and structural changes in the thylakoid membrane (Pospíšil, 2016). ROS cause inactivation of the PSII reaction-center proteins (e.g. Yamane *et al.*, 1998; Yoshioka *et al.*, 2006) as well as inhibition of *de novo* protein synthesis (Allakhverdiev *et al.*, 2008). In addition, ROS production under high T_{leaf} has been shown to suppress non-photochemical quenching, which affords the leaf protection under moderate heating (Hideg *et al.*, 2008) and may explain the observed full recovery from less severe heat stress (Fig. 6). We note, however, that leaves of trees growing under field conditions in the tropics often will be exposed to continuous high irradiance, or recurring transient sun flecks, and will thus exist in a semipermanent state of daytime heat-induced PSII suppression with a longer recovery period during the night. Therefore, although protocols utilizing instantaneous measurements may underestimate the threshold temperatures for permanent PSII damage (Krause *et al.*, 2010), they do directly inform about a loss in photosynthetic capacity that reduces plant carbon uptake.

Conclusions

Plants can handle temperature extremes by two broad strategies: tolerance and avoidance. We used three tropical montane tree species with different growth and water use strategies to study among-species differences in heat stress exposure, intensity and acclimation capacity. High heat tolerance was linked to both interspecific differences in leaf osmolality and plasticity in thylakoid membrane lipid composition. However, we also found that latent cooling of leaves by high transpiration rates was the more effective strategy for avoiding heat stress, as it resulted in wider TSMs at all sites and thus reduced the need for high heat tolerance. This suggests that montane climax species, with large leaves and low transpiration rates resulting in high T_{leaf}, may be especially susceptible for photosynthetic heat stress under warming climate. However, because warming is commonly accompanied with intensification of droughts, which is likely to reduce transpiration rates, future field studies should explore the role of heat and drought interactions in causing heat stress in different species to further evaluate which strategy is more advantageous on longer timescales. Furthermore, our results suggest that once systematic, species-specific evaluations of photosynthetic heat tolerance have been made on a wider array of species, trait-based approaches may be able to predict a species' heat stress exposure, intrinsic thermal tolerance and heat acclimation potential.

Acknowledgements

We are thankful for the support provided by the Swedish Research Council (VR; grant no. 2015-03338), the Swedish Research Council for Environmental, Agricultural Science and Spatial Planning (Formas; grant no. 2015-1458), and the Swedish strategic research area 'Biodiversity and Ecosystem services in a Changing Climate' (BECC; https://www.lu.se). We are grateful to the Rwanda Agriculture and Animal Resources Development Board for providing the sites for the Rwanda-TREE experiment (https://www.rwandatree.com/). LT gratefully acknowledges funding from the Swedish Research Council for Environmental, Agricultural Science and Spatial Planning (Formas: grant no. 2019-01470).

Author contributions

JU suggested the topic; LT, MW, GW and JU designed the experiment; LT, MW and EZ carried out the field chlorophyll fluorescence measurements; MM provided leaf gas exchange and leaf temperature data; AM provided leaf morphology data; BN, EZ and GW established and managed the field sites; LT, CR and OJLM carried out the laboratory-based chlorophyll fluorescence measurements; MXA analyzed the thylakoid membrane lipids; CS provided advice regarding the chlorophyll fluorescence method and discussion of the data; DN, GW and JU supervised the field work; and LT analyzed the data and wrote the manuscript. All authors contributed to the editing of the manuscript and approved the final version.

ORCID

Mats X. Andersson https://orcid.org/0000-0003-4279-6572
Olivier J. L. Manzi https://orcid.org/0000-0002-5255-5652
Cornelia Spetea https://orcid.org/0000-0001-7609-0290
Lasse Tarvainen https://orcid.org/0000-0003-3032-9440
Johan Uddling https://orcid.org/0000-0003-4893-1915
Göran Wallin https://orcid.org/0000-0002-5359-1102
Maria Wittemann https://orcid.org/0000-0002-3323-1556
Etienne Zibera https://orcid.org/0000-0003-1983-7030

Data availability

The data that supports the findings of this study are available in the supplementary material of this article (Dataset S1).

© 2021 The Authors
New Phytologist © 2021 New Phytologist Foundation

References

Aleixo I, Norris D, Hemerik L, Barbosa A, Prata E, Costa F, Poorter L. 2019. Amazonian rainforest tree mortality driven by climate and functional traits. *Nature Climate Change* **9**: 384–388.

Allakhverdiev SL, Kreslavski VD, Klimov VV, Los DA, Carpentier R, Mphanty P. 2008. Heat stress: an overview of molecular responses in photosynthesis. *Photosynthesis Research* **98**: 541–550.

Allen CD, Macalady AK, Chenchouni H, Bachelet D, McDowell N, Vennetier M, Kitzberger T, Rigling A, Breshears DD, Hogg EH *et al.* 2010. A global overview of drought and heat-induced tree mortality reveals emerging climate change risks for forests. *Forest Ecology and Management* **259**: 660–684.

Araújo I, Marimon BS, Scalon MC, Fauset S, Marimon Junior BH, Tiwari R, Galbraith DR, Gloor MU. 2021. Trees at the Amazonia-Cerrado transition are approaching high temperature thresholds. *Environmental Research Letters* **16**: 034047.

Aspinwall MJ, Pfautsch S, Tjoelker MG, Vårhammar A, Possell M, Drake JE, Reich PB, Tissue DT, Atkin OK, Rymer PD *et al.* 2019. Range size and growth temperature influence *Eucalyptus* species responses to an experimental heatwave. *Global Change Biology* **25**: 1665–1684.

Bartlett MK, Scoffoni C, Ardy R, Zhang Y, Sun S, Cao K, Sack L. 2012. Rapid determination of comparative drought tolerance traits: using an osmometer to predict turgor loss point. *Methods in Ecology and Evolution* **3**: 880–888.

Barua D, Downs CA, Heckathorn SA. 2003. Variation in chloroplast small heat-shock protein function is a major determinant of variation in thermotolerance of photosynthetic electron transport among ecotypes of *Chenopodium album*. *Functional Plant Biology* **30**: 1071–1079.

Battisti DS, Naylor RL. 2009. Historical warnings of future food insecurity with unprecedented seasonal heat. *Science* **323**: 240–244.

Berry J, Björkman O. 1980. Photosynthetic response and adaptation to temperature in higher plants. *Annual Review of Plant Physiology* **31**: 491–543.

Bilger H-W, Schreiber U, Lange OL. 1984. Determination of leaf heat resistance: comparative investigation of chlorophyll fluorescence changes and tissue necrosis methods. *Oecologia* **63**: 256–262.

Bloesch U, Troupin G, Derungs N. 2009. *Les plantes ligneuses du Rwanda: flore, ecologie et usages*. Düren, Germany: Shaker Verlag.

Campbell GS, Norman JM. 1998. *An introduction to environmental biophysics, 2nd edn*. New York, NY, USA: Springer.

Claeys F, Gourlet-Fleury S, Picard N, Ouédraogo D-Y, Tadesse MG, Hérault B, Baya F, Bénédet F, Cornu G, Mortier F. 2019. Climate change would lead to a sharp acceleration of central African forests dynamics by the end of the century. *Environmental Research Letters* **14**: 044002.

Coumou D, Robinson A, Rahmstorf S. 2013. Global increase in record-breaking monthly-mean temperatures. *Climatic Change* **118**: 771–782.

Cunningham SC, Read J. 2003. Do temperate rainforest trees have a greater ability to acclimate to changing temperatures than tropical rainforest trees? *New Phytologist* **157**: 55–64.

Curtis EM, Knight CA, Leigh A. 2019. Intracanopy adjustment of leaf-level thermal tolerance is associated with microclimatic variation across the canopy of a desert tree (*Acacia papyrocarpa*). *Oecologia* **189**: 37–46.

Curtis EM, Knight CA, Petrou K, Leigh A. 2014. A comparative analysis of photosynthetic recovery from thermal stress: a desert plant case study. *Oecologia* **175**: 1051–1061.

Diffenbaugh NS, Scherer M. 2011. Observational and model evidence of global emergence of permanent, unprecedented heat in the 20th and 21st centuries. *Climatic Change* **107**: 615–624.

Doughty CE, Goulden ML. 2008. Are tropical forests near a high temperature threshold? *Journal of Geophysical Research* **113**: G00B07.

Drake JE, Tjoelker MG, Vårhammar A, Medlyn B, Reich PB, Leigh A, Pfautsch S, Blackman CJ, López R, Aspinwall MJ *et al.* 2018. Trees tolerate an extreme heatwave via sustained transpirational cooling and increased leaf thermal tolerance. *Global Change Biology* **24**: 2390–2402.

Duque A, Stevenson PR, Feeley KJ. 2015. Thermophilization of adult and juvenile tree communities in the northern tropical Andes. *Proceedings of the National Academy of Sciences, USA* **112**: 10744–10749.

Fadrique B, Báez S, Duque Á, Malizia A, Blundo C, Carilla J, Osinaga-Acosta O, Malizia L, Silman M, Farfán-Ríos W *et al.* 2018. Widespread but heterogeneous responses of Andean forests to climate change. *Nature* **564**: 207–212.

Fauset S, Freitas HC, Galbraith DR, Sullivan MJP, Aidar MPM, Joly CA, Phillips OL, Vieira SA, Gloor MU. 2018. Differences in leaf thermoregulation and water use strategies between three co-occurring Atlantic forest tree species. *Plant, Cell & Environment* **41**: 1618–1631.

Feeley K, Martinez-Villa J, Perez T, Silva Duque A, Triviño Gonzalez D, Duque A. 2020. The thermal tolerances, distributions, and performances of tropical montane tree species. *Frontiers in Forests and Global Change* **3**: 25.

Feeley KJ, Silman MR, Bush MB, Farfan W, Carcia Gabrera K, Malhi Y, Meir P, Salinas Revilla N, Natividad Raurau Quisiyupanqui M, Saatchi S. 2011. Upslope migration of Andean trees. *Journal of Biogeography* **38**: 783–791.

Hideg É, Kós PB, Schreiber U. 2008. Imaging of NPQ and ROS formation in tobacco leaves: heat inactivation of the water–water cycle prevents down-regulation of PSII. *Plant & Cell Physiology* **49**: 1879–1886.

Hüve K, Bichele I, Rasulov B, Niinemets Ü. 2011. When it is too hot for photosynthesis: heat-induced instability of photosynthesis in relation to respiratory burst, cell permeability changes and H_2O_2 formation. *Plant, Cell & Environment* **34**: 113–126.

Hüve K, Bichele I, Tobias M, Niinemets Ü. 2006. Heat sensitivity of photosynthetic electron transport varies during the day due to changes in sugars and osmotic potential. *Plant, Cell & Environment* **29**: 212–228.

Janzen DH. 1967. Why mountain passes are higher in the tropics. *American Naturalist* **101**: 233–249.

Knight CA, Ackerly DD. 2002. An ecological and evolutionary analysis of photosynthetic thermotolerance using the temperature-dependent increase in fluorescence. *Oecologia* **130**: 505–514.

Knight CA, Ackerly DD. 2003. Evolution and plasticity of photosynthetic thermal tolerance, specific leaf area and leaf size: congeneric species from desert and coastal environments. *New Phytologist* **160**: 337–347.

Kourtchenko O, Andersson MX, Hamberg M, Brunnström Å, Göbel C, McPhail KL, Gerwick WH, Feussner I, Ellerström M. 2007. Oxo-phytodienoic acid-containing galactolipids in arabidopsis: jasmonate signaling dependence. *Plant Physiology* **145**: 1658–1669.

Krause GH, Winter K, Krause B, Jahns P, García M, Aranda J, Virgo A. 2010. High-temperature tolerance of a tropical tree, *Ficus insipida*: methodological reassessment and climate change considerations. *Functional Plant Biology* **37**: 890–900.

't Lam RUE. 2010. Scrutiny of variance results for outliers: Cochran's test optimized. *Analytica Chimica Acta* **659**: 68–84.

Leigh A, Sevanto S, Ball MC, Close JD, Ellsworth DS, Knight CA, Nicotra AB, Vogel S. 2012. Do thick leaves avoid thermal damage in critically low wind speeds? *New Phytologist* **194**: 477–487.

Mathur S, Agrawal D, Jajoo A. 2014. Photosynthesis: response to high temperature stress. *Journal of Photochemistry and Photobiology B: Biology* **137**: 116–126.

Maxwell K, Johnson GN. 2000. Chlorophyll fluorescence – a practical guide. *Journal of Experimental Botany* **51**: 659–668.

Michaletz ST, Weiser MD, McDowell NG, Zhou J, Kaspari M, Helliker BR, Enquist BJ. 2016. The energetic and carbon economic origins of leaf thermoregulation. *Nature Plants* **2**: 16129.

Michaletz ST, Weiser MD, Zhou J, Kaspari M, Helliker BR, Enquist BJ. 2015. Plant thermoregulation: energetics, trait–environment interactions, and carbon economics. *Trends in Ecology & Evolution* **30**: 714–724.

Mujawamariya M, Wittemann M, Manishimwe A, Ntirugulirwa B, Zibera E, Nsabimana D, Wallin G, Uddling J, Dusenge ME. 2021. Complete or overcompensatory thermal acclimation of leaf dark respiration in African tropical trees. *New Phytologist* **229**: 2548–2561.

Murchie EH, Lawson T. 2013. Chlorophyll fluorescence analysis: a guide to good practice and understanding some new applications. *Journal of Experimental Botany* **64**: 3983–3998.

Niinemets Ü. 2018. When leaves go over the thermal edge. *Plant, Cell & Environment* **41**: 1247–1250.

Nilsson AK, Johansson ON, Fahlberg P, Steinhart F, Gustavsson MB, Ellerström M, Andersson MX. 2014. Formation of oxidized phosphatidylinositol and 12-oxo-phytodienoic acid containing acylated

© 2021 The Authors
New Phytologist © 2021 New Phytologist Foundation

phosphatidylglycerol during the hypersensitive response in Arabidopsis. *Phytochemistry* **101**: 65–75.

Nilsson AK, Sjöbom U, Christenson K, Hellström A. 2019. Lipid profiling of suction blister fluid: comparison of lipids in interstitial fluid and plasma. *Lipids in Health and Disease* **18**: 1–11.

Ntawuhiganayo EB, Uwizeye FK, Zibera E, Dusenge ME, Ziegler C, Ntirugulirwa B, Nsabimana D, Wallin G, Uddling J. 2020. Traits controlling shade tolerance in tropical montane trees. *Tree Physiology* **40**: 183–197.

O'sullivan OS, Heskel MA, Reich PB, Tjoelker MG, Weerasinghe LK, Penillard A, Zhu L, Egerton JJG, Bloomfield KJ, Creek D *et al.* 2017. Thermal limits of leaf metabolism across biomes. *Global Change Biology* **23**: 209–223.

Pau S, Detto M, Kim Y, Still CJ. 2018. Tropical forest temperature thresholds for gross primary productivity. *Ecosphere* **9**: e02311.

Perez TM, Feeley KJ. 2020. Photosynthetic heat tolerances and extreme leaf temperatures. *Functional Ecology* **34**: 2236–2245.

Perkings-Kirkpatrick SE, Lewis SC. 2020. Increasing trends in regional heatwaves. *Nature Communications* **11**: 3357.

Phillips OL. 1997. The changing ecology of tropical forests. *Biodiversity and Conservation* **6**: 291–311.

Pollastrini S, Jorba I, Hawkins TJ, Llusià J, Michelozzi M, Navajas D, Peñuelas J, Hussey PJ, Knight MR, Loreto F. 2019. Leaves of isoprene-emitting tobacco plants maintain PSII stability at high temperatures. *New Phytologist* **223**: 1307–1318.

Pospíšil P. 2016. Production of reactive oxygen species by photosystem ii as a response to light and temperature stress. *Frontiers in Plant Science* **7**: 1950.

Reich PB. 2014. The world-wide 'fast–slow' plant economics spectrum: a traits manifesto. *Journal of Ecology* **102**: 275–301.

Rodrigues TB, Baker CR, Walker AP, McDowell N, Rogers A, Higuchi N, Chambers JQ, Jardine KJ. 2020. Stimulation of isoprene emissions and electron transport rates as key mechanisms of thermal tolerance in the tropical species *Vismia guianensis*. *Global Change Biology* **26**: 5928–5941.

Rosado BHP, Joly CA, Burgess SSO, Oliveira RS, Aidar MPM. 2016. Changes in plant functional traits and water use in Atlantic rainforest: evidence of conservative water use in spatio-temporal scales. *Trees* **30**: 47–61.

Santarius KA. 1973. The protective effect of sugars on chloroplast membranes during temperature and water stress and its relationship to frost, desiccation and heat resistance. *Planta* **113**: 105–114.

Sastry A, Barua D. 2017. Leaf thermotolerance in tropical trees from a seasonally dry climate varies along the slow-fast resource acquisition spectrum. *Scientific Reports* **7**: 11246.

Sharkey TD. 2005. Effects of moderate heat stress on photosynthesis: importance of thylakoid reactions, rubisco deactivation, reactive oxygen species, and thermotolerance provided by isoprene. *Plant, Cell & Environment* **28**: 269–277.

Slot M, Cala D, Aranda J, Virgo A, Michaletz ST, Winter K. 2021. Leaf heat tolerance of 147 tropical forest species varies with elevation and leaf functional traits, but not with phylogeny. *Plant, Cell & Environment* **44**: 2414–2427.

Slot M, Krause HG, Krause B, Hernández GG, Winter K. 2019. Photosynthetic heat tolerance of shade and sun leaves of three tropical species. *Photosynthesis Research* **141**: 119–130.

Sullivan MJP, Lewis SL, Affum-Baffoe K, Castilho C, Costa F, Cuni Sanchez A, Ewango CEN, Hubau W, Marimon B, Monteagudo-Mendoza A *et al.* 2020. Long-term thermal sensitivity of Earth's tropical forests. *Science* **368**: 869–874.

Taylor TC, Smith MN, Slot M, Feeley KJ. 2019. The capacity to emit isoprene differentiates the photosynthetic temperature responses of tropical plant species. *Plant, Cell & Environment* **42**: 2448–2457.

Teskey R, Wertin T, Bauweraerts I, Ameye M, McGuire MA, Steppe K. 2015. Responses of tree species to heat waves and extreme heat events. *Plant, Cell & Environment* **38**: 1699–1712.

Tiwari R, Gloor E, da Cruz WJA, Schwantes Marimon B, Marimon-Junior BH, Reis SM, de Souza IA, Krause HG, Slot M, Winter K *et al.* 2021. Photosynthetic quantum efficiency in south-eastern Amazonian trees may be already affected by climate change. *Plant, Cell & Environment* **44**: 2428–2439.

Toomey M, Roberts DA, Still C, Goulden ML, McFadden JP. 2011. Remotely sensed heat anomalies linked with Amazonian forest biomass declines. *Geophysical Research Letters* **38**: L19704.

Tserej O, Feeley KJ. 2021. Variation in leaf temperatures of tropical and subtropical trees are related to leaf thermoregulatory traits and not geographic distributions. *Biotropica* **53**: 868–878.

Vierling E. 1991. The role of heat shock proteins in plants. *Annual Review of Plant Physiology and Plant Molecular Biology* **42**: 579–620.

Wang H, Prentice IC, Davis TW, Keenan TF, Wright IJ, Peng C. 2017. Photosynthetic responses to altitude: an explanation based on optimality principles. *New Phytologist* **213**: 976–982.

Watson KM. 1943. Thermodynamics of the liquid states – generalized prediction of properties. *Industrial and Engineering Chemistry* **35**: 398–406.

Wright IJ, Dong N, Maire V, Prentice IC, Westoby M, Díaz S, Gallagher RV, Jacobs BF, Kooyman R, Law EA *et al.* 2017. Global climatic drivers of leaf size. *Science* **357**: 917–921.

Wright IJ, Reich PB, Westoby M, Ackerly DD, Baruch Z, Bongers F, Cavender-Bares J, Chapin T, Cornelissen JHC, Diemer M *et al.* 2004. The worldwide leaf economics spectrum. *Nature* **428**: 821–827.

Yamamoto Y. 2016. Quality control of photosystem II: the mechanisms for avoidance and tolerance of light and heat stresses are closely linked to membrane fluidity of the thylakoids. *Frontiers in Plant Science* **7**: 1136.

Yamane Y, Kashino Y, Koike H, Satoh K. 1998. Effects of high temperatures on the photosynthetic systems in spinach: oxygen-evolving activities, fluorescence characteristics and the denaturation process. *Photosynthesis Research* **57**: 51–59.

Yoshioka M, Uchida S, Mori J, Komayama K, Ohira S, Morita N, Nakanishi T, Yamamoto Y. 2006. Quality control of photosystem II. Cleavage of reaction center D1 protein in spinach thylakoids by FtsH protease under moderate heat stress. *Journal of Biological Chemistry* **281**: 21660–21669.

Zhu L, Bloomfield KJ, Hocart CH, Egerton JJG, O'Sullivan OS, Penillard A, Weerasinghe LK, Atkin OK. 2018. Plasticity of photosynthetic heat tolerance in plants adapted to thermally contrasting biomes. *Plant, Cell & Environment* **41**: 1251–1262.

Supporting Information

Additional Supporting Information may be found online in the Supporting Information section at the end of the article.**Dataset S1** The data used in the study.

Fig. S1 Determination of the T_{crit} by piecewise linear regression.

Fig. S2 Determination of the threshold temperatures for F_v/F_m reduction (T_{20} and T_{50}) using the Gompertz function.

Fig. S3 Image of the heating set up used during the field measurements.

Fig. S4 Meteorological conditions during the field campaign.

Fig. S5 Midday temperatures of sunlit leaves in February 2019.

Fig. S6 Correlations between T_{crit}, T_{20} and T_{50}, and the average number of double bonds.

Fig. S7 Photosynthetic heat tolerance thresholds in chamber-grown *H. montana* seedlings.

Methods S1 Description of the laboratory-based chlorophyll fluorescence measurements.

Methods S2 Determination of leaf temperature using the energy balance approach.

© 2021 The Authors
New Phytologist © 2021 New Phytologist Foundation

Table S1 Tree heights, and leaf lengths, widths and angles at the three study sites.

Table S2 Statistical summary.

Table S3 Statistical comparison of the among-sites and -species differences in T_{crit} with Welch's *t*-test.

Table S4 Statistical comparison of the among-sites and -species differences in T_{20} with Welch's *t*-test.

Table S5 Statistical comparison of the among-sites and -species differences in T_{50} with Welch's *t*-test.

Please note: Wiley Blackwell are not responsible for the content or functionality of any Supporting Information supplied by the authors. Any queries (other than missing material) should be directed to the *New Phytologist* Central Office.



About *New Phytologist*

- *New Phytologist* is an electronic (online-only) journal owned by the New Phytologist Foundation, a **not-for-profit organization** dedicated to the promotion of plant science, facilitating projects from symposia to free access for our Tansley reviews and Tansley insights.
- Regular papers, Letters, Viewpoints, Research reviews, Rapid reports and both Modelling/Theory and Methods papers are encouraged. We are committed to rapid processing, from online submission through to publication 'as ready' via *Early View* – our average time to decision is <26 days. There are **no page or colour charges** and a PDF version will be provided for each article.
- The journal is available online at Wiley Online Library. Visit **www.newphytologist.com** to search the articles and register for table of contents email alerts.
- If you have any questions, do get in touch with Central Office (np-centraloffice@lancaster.ac.uk) or, if it is more convenient, our USA Office (np-usaoffice@lancaster.ac.uk)
- For submission instructions, subscription and all the latest information visit **www.newphytologist.com**

© 2021 The Authors
New Phytologist © 2021 New Phytologist Foundation